$CeAlO_3$ formation has been proposed by Kaufherr et al.[8] The fact that higher reduction temperature is required for the large CeO_2 particles to form $CeAlO_3$ is probably due to diffusional limitations of Ce to form the solid solution with alumina. As also shown in TPR, during the formation of $CeAlO_3$ from the large CeO_2 particles, the CeO_x phases (Ce_2O_3 when reduction temperature is above 800 °C) are formed. Some portions of the CeO_x species may form the solid solution with alumina, and the remaining CeO_x species are reoxidized to CeO_2 when exposed to ambient air before XPS analysis. It appears that formation of $CeAlO_3$ from CeO_2 particles (both small crystallites and large particles) on alumina involves an intermediate state in which ceria is, at least, partially reduced.

5. Conclusions

Surface characterization of CeO_2/Al_2O_3 by XPS, Raman spectroscopy, and TPR leads to the following conclusions:

1. Three ceria phases can be found on CeO_2/Al_2O_3, depending on ceria loading. These phases are the $CeAlO_3$ precursor, intermediate (small crystallite, not detectable by XRD), and large CeO_2 particles (≅20 nm in size).

2. The $CeAlO_3$ precursor shows a Ce(III)-like feature in XPS and gives a completely different spectrum from CeO_2 in Raman scattering experiments, while TPR data reveal that this Ce species is more easily reduced into $CeAlO_3$ than the CeO_2 particles on alumina.

3. Ceria in the $CeAlO_3$ precursor and in a small crystallite form on alumina can be transformed into $CeAlO_3$, upon reduction in H_2 at temperatures higher than 600 °C, while even a partial conversion to $CeAlO_3$ from the large CeO_2 particles requires a temperature above ≅800 °C.

4. $CeAlO_3$, formed by reduction of CeO_2/Al_2O_3, shows good thermal stability in air in the temperature range up to 600 °C.

Note Added in Proof. Further studies of the γ-alumina material used in this work indicate that some of the Raman lines assigned to the dispersed phase of Ceria may be due to transitional alumina phases instead.

Acknowledgment. We acknowledge the following colleagues at Ford Research: R. K. Belitz for XRD analysis; R. J. Baird, G. W. Graham, M. Bettman, and K. Otto for useful discussions; L. C. Davis for useful information regarding the theoretical aspects in photoemission of Ce oxides; and M. Shelef for a review of the manuscript and helpful discussions. Also, a useful discussion with Professor John C. Hemminger of the University of California, Irvine, is acknowledged.

Molecular Orbital Study of Nickel–Oxygen Interactions

Henry Castejón, Antonio J. Hernández,

Departamento de Química, Universidad Simón Bolívar, Apartado 80659, Caracas 1080-A, Venezuela

and Fernando Ruette*

Centro de Química, Instituto Venezolano de Investigaciones Científicas, IVIC, Apartado 21827, Caracas 1010-A, Venezuela *(Received: October 12, 1987)*

A modified CNDO-UHF procedure is used to study nickel–oxygen interactions in NiO and $[NiO_2]^q$ (q = 0, 2+) systems. Some relevant properties are compared with those obtained in a previous study on analogous cobalt–oxygen adducts. The nickel orbitals that most contribute to the bonding in these molecules are the 4s and 3d, with relatively little contribution from the 4p orbitals. The ground state of NiO is calculated to be a $^3\Sigma$ with π holes localized in Ni(3d) orbitals. The most stable deformation state for the $[NiO_2]^0$ system corresponded to a peroxo $^1A_1$ state with a $^1A'$ superoxo state 10 kcal/mol higher in energy. This is reversed in the $[NiO_2]^{2+}$ system, where a superoxo $^1A'$ state is the most stable distortion geometry. The dioxygen activation, measured by Boca's $\chi(\pi)$ index, in these O_2 adducts decreased when the oxidation state of nickel increased from Ni(0) to Ni(II). The lowest activation energy calculated to break the O–O bond corresponded to 112 kcal/mol, suggesting a nondissociative chemisorption of O_2 on a single Ni atom.

Introduction

In a previous paper[1] we reported CNDO-UHF calculations for the distortion, dioxygen activation, and dissociation properties of $[CoO_2]^q$ as a preliminary step in the calculation of the properties of O_2 on transition metals anchored to metal oxides[2,3] and metallic surfaces.[4] Dioxygen complexes of this type have recently become of considerable interest to chemists because of their importance for both homogeneous and heterogeneous catalysis. We studied the effect of the net charge q on the stabilization of the electronic states of the adduct to simulate the interaction of transition metals with different kinds of chemical environments. The results obtained clearly showed that one may accurately study the behavior of a given electronic state along the distortion and dissociation coordinates using semiempirical methods. They constitute an adequate framework for the explanation of experimental data provided that the state of minimum energy is fixed along the reaction path.

TABLE I: Parameters for Nickel and Oxygen

orbital μ	$-^1/_2(I_\mu + A_\mu)$, eV	ξ_μ	$-\beta^\circ_\mu$, eV
	nickel		
4s	4.306[a]	2.55	5.0
4p	1.260[a]	1.05	3.0
3d	6.182[a]	2.95	8.5
	oxygen		
2s	25.39017[b]	2.275[b]	23.0
2p	9.111[b]	2.275[b]	22.3

[a] Reference 11. [b] Reference 12.

In the present work we report similar studies on $[NiO_2]^q$, where we have chosen q = 0 and 2+ as the representative cases. Experimental data show that binary dioxygen complexes of nickel are capable of existing under conditions of matrix isolation.[5] The poor CNDO estimates of the binding energies are improved by an adequate parametrization that reproduces the equilibrium bond lengths and bond energies of O_2 and NiO. This thermodynamic

(1) Hernández, A.; Ruette, F.; Ludeña, E. V. *J. Mol. Catal.* **1987**, *39*, 21.
(2) Beran, S.; Jiru, P.; Wichterlova, B. *J. Phys. Chem.* **1981**, *85*, 1951.
(3) Ruette, F.; Ludeña, E. V. *J. Catal.* **1981**, *67*, 266.
(4) Ruette, F.; Hernández, A.; Ludeña, E. V. *Surf. Sci.* **1985**, *151*, 103.
(5) Huber, H.; Ozin, G. A. *Can. J. Chem.* **1972**, *50*, 3746.

0022-3654/88/2092-4970$01.50/0

TABLE II: NiO and O_2 Bonding Properties

molecule	orbital occupancies: Ni s	Ni p	Ni d	O s	O p	Mulliken bond order: sp–sp	sp–d	bond length,[a] Å	binding energy,[a] kcal/mol
$NiO(^{3(1)}\Sigma)^b$	0.85	0.13	8.73	1.86	4.43	0.76	0.16	1.61 (1.67)[c]	98.1 (90)[d]
$O_2(^{3(1)}\Sigma)^b$				1.88	4.12	1.31		1.205 (1.207)[e]	118.6 (118.1)[e]

[a] Values in parentheses represent experimental values. [b] $^3\Sigma$ and $^1\Sigma$ are degenerate states in CNDO. [c] Configuration interaction calculations from ref 13. [d] Reference 14. [e] Reference 12.

fitting has been discussed recently with regard to the applications of semiempirical methods to transition metals.[1,6-9] In the next section we briefly describe the CNDO-UHF method used and the parametrization. Later, we discussed the thermodynamic and dioxygen activation properties of the most stable electronic states of $[NiO_2]^q$ (q = 0, 2+) as function of the distortion and dissociation angles, where some relevant bonding properties are compared with those obtained in a previous study of cobalt–oxygen interactions.[1] Concluding remarks are presented in the last section.

Parametrization

The calculations were done with a semiempirical UHF-CNDO method that is a modification of the QCPE-290 algorithm described by Rinaldi.[10] The details of the method as well as its ability to search for the most stable electronic state at any given molecular geometry and maintain it along the deformation and dissociation reaction coordinates have been discussed previously.[1]

The selected Slater coefficients ξ_μ and bonding parameters β°_μ (μ = s, p, d) are listed in Table I. They were chosen to reproduce the experimental bond energies and equilibrium bond lengths of NiO and O_2. The Ni($4s^1$,$3d^7$) configuration corresponds to the ground state calculated with the parameters listed in Table I. The calculated bonding properties of the ground state of NiO and O_2 are presented in Table II. The most stable configuration calculated for NiO corresponded to a $^{3(1)}\Sigma$ state ($^3\Sigma$ and $^1\Sigma$ are degenerate states in CNDO) with a hole in a π orbital localized on Ni(d_π) and gross atomic population 4s (0.85), 4p (0.13), 3d (8.73). The relatively low Ni(4p) orbital occupancy and the fact that its orbital mixing is never larger than 3% indicate its relatively small contribution to the bonding in NiO. The calculated $NiO(^3\Sigma)$ bond length and binding energy corresponded to 1.61 Å and 98.1 kcal/mol, respectively. We chose the neutral nickel and oxygen atoms as the dissociation limit in the present binding energy calculation mainly because the population analysis of this state (see orbital occupancies in Table II) indicated rather low gross charges of about Ni(0.3+) and O(0.3–). All the above results are in close agreement with previous GBV ab initio calculations.[15]

Recent ASED-MO results of Anderson et al.[9] and ab initio configuration interaction calculations of Bauschlicher et al.[13] also predicted a $NiO(^3\Sigma)$ electronic ground state with estimated equilibrium bond distance of about 1.66–1.67 Å, although this value was considered too long[13] (the experimental value is unknown). These authors assigned a large ionic character to the NiO bond. In fact, Mulliken population analysis gave a negative charge of about 0.7 electron for oxygen in NiO,[13] which is far from the 0.3 electronic transfer to oxygen found in the present study. Taking into account the NiO charge-transfer properties at equilibrium, the ASED-MO semiempirical theory of Anderson et al.[9] also describes a rather ionic NiO bond. The value of 0.16

TABLE III: Distortion States of NiO_2

state[a]	configuration	bond length,[b] Å: Ni–O	O–O	total energy, au	charge on O_2, e
		$[NiO_2]^0$			
$^1A_1$	α-$5a_1^2a_2^2b_1^2b_2$ β-$5a_1^2a_2^2b_1^2b_2$	1.70	1.28	−73.6030	−0.344
$^3A_2$	α-$5a_1^2a_2^3b_1^2b_2$ β-$5a_1^2a_2^2b_1^1b_2$	1.72	1.29	−73.5931	−0.339
$^1A'$	α-6a′5a′ β-7a′4a″	1.62	1.29	−73.5870	−0.337
$^3A'$	α-7a′5a″ β-7a′3a″	1.60	1.29	−73.5854	−0.317
		$[NiO_2]^{2+}$			
$2^1A'$	α-4a′6a″ β-4a′6a″	1.64	1.23	−72.2432	+0.592
1^1A_1	α-$4a_1^2a_2^2b_1^2b_2$ β-$4a_1^2a_2^2b_1^2b_2$	1.78	1.25	−72.2294	+0.529
$^3A_2$	α-$5a_1^2a_2^2b_1^2b_2$ β-$4a_1^1a_2^2b_1^2b_2$	1.79	1.25	−72.2159	+0.533
$^3A''$	α-6a′5a″ β-5a′4a″	1.66	1.26	−72.2148	+0.564

[a] C_{2v} designation is used for the peroxo and C_s for the superoxo states. [b] Only the smallest Ni–O distance is reported.

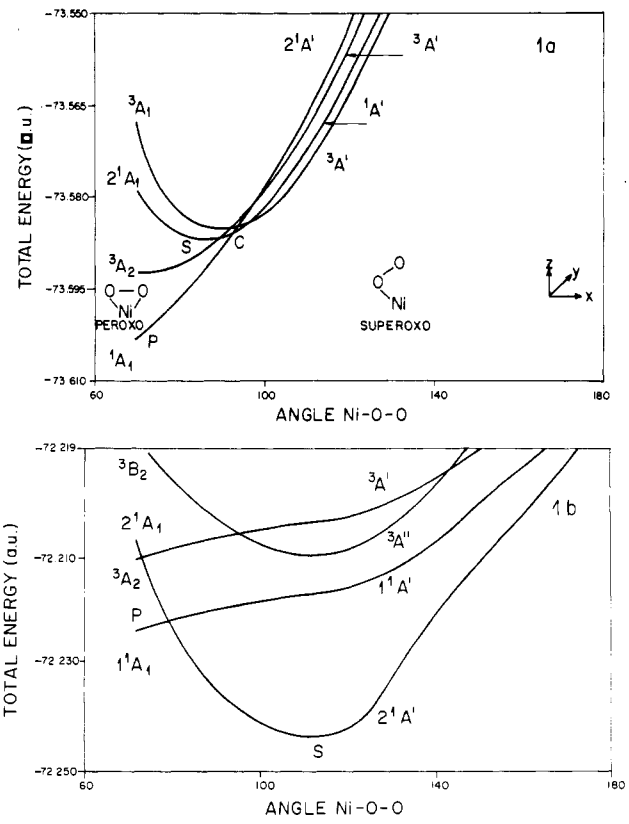

Figure 1. Energy of $[NiO_2]^q$ as a function of the Ni–O–O bond angle for the states listed in Table III, distortion curves for (a) q = 0, (b) q = 2+.

(6) Ruette, F.; Hernández, A.; Ludeña, E. V. *Int. J. Quantum Chem.* **1986**, *29*, 1351.
(7) Blyholder, G.; Head, J.; Ruette, F. *Theor. Chim. Acta* **1982**, *60*, 429.
(8) Ruette, F.; Ludeña, E. V.; Hernández, A.; Castro, G. *Surf. Sci.* **1986**, *167*, 393.
(9) Anderson, A. B.; Grimes, R. W.; Hong, S. Y. *J. Phys. Chem.* **1987**, *91*, 4225.
(10) Rinaldi, D. *Comput. Chem.* **1976**, *1*, 109.
(11) Clack, D. W.; Hush, N. S.; Yandle, J. R. *J. Chem. Phys.* **1972**, *57*, 3503.
(12) Pople, J. A.; Beveridge, D. *Approximate Molecular Orbital Theory*; McGraw-Hill: New York, 1970.
(13) Bauschlicher, C. W., Jr.; Nelin, C. J.; Bagus, P. S. *J. Chem. Phys.* **1985**, *82*, 3265.
(14) Huber, K. P.; Herzberg, G. *Molecular Spectra and Molecular Structure IV. Constants of Diatomic Molecules*; Van Nostrand: New York, 1979.
(15) Walch, S. P.; Goddard, W. A., III *J. Am. Chem. Soc.* **1978**, *100*, 1338.

for the sp–d Mulliken (overlap weighted) bond order shown in Table II indicates a small participation of the Ni(3d) orbitals, although they seem to play an important role in the NiO bonding properties.[13]

Distortion Properties of $[NiO_2]^q$

Calculations with optimization of geometry for the most stable electronic states in different geometric arrangements, ranging from the side-bonded to the linear-bonded NiO_2, were carried out. The distortion energy curves for the lowest electronic states of both peroxo and superoxo structures of $[NiO_2]^q$ ($q = 0, 2+$) are shown in Figure 1, parts a and b, respectively. Here, the Ni–O–O angle was chosen as the deformation coordinate, i.e., the Ni–O and O–O bond distances were optimized at each angle studied. The corresponding bond lengths, total energies, and charge on O_2, calculated at the minimum of the distortion energy potential curves, are given in Table III. The distortion curves depicted in Figure 1a show peroxo and superoxo states that are represented by the symbols P and S, respectively. The point P corresponds to the minimum of the dissociation potential energy curve for the most stable peroxo state ($^1A_1$): see the next two sections. The most stable geometry for the $[NiO_2]^0$ system corresponds to a peroxo $^1A_1$ state, with a $^1A'$ superoxo state about 10 kcal/mol higher in energy. This is in agreement with the low-temperature (argon matrices at 4.2–10.0 K) experimental data of Huber and Ozin,[5] which show that the dioxygen molecule is coordinated to the nickel atom in a sideways fashion in $[NiO_2]^0$. Recent ab initio configuration interaction calculations of Blomberg et al.[16] also predicted a peroxo $^1A_1$ ground state for the neutral Ni–O_2 adduct as the preferred geometry. They estimated Ni–O and O–O equilibrium bond distances of 2.22 and 1.40 Å, respectively, and a 0.56 electronic charge transfer to O_2, which is far from the 0.34 value found in this work. This increase in the O_2 electronic population causes a larger O_2 weakening as indicated by the substancial O–O bond length increase from 1.28 Å in the present work to the 1.40-Å value reported in ref 16. As pointed out in the previous section, our CNDO parametrization scheme underestimates the large ionic character of the NiO bonds. Inclusion of the equilibrium charge-transfer properties predicted from the difference in electronegativity of nickel and oxygen[9] in our parametrization scheme remains to be investigated. The energy barrier (E_a) for the peroxo to superoxo transformation (path P → C → S in Figure 1a) is 13 kcal/mol. As indicated in Figure 1b, this situation is reversed in the $[NiO_2]^{2+}$ system. Here, the superoxo 2^1A state, with distortion of the Ni–O–O angle of about 115°, corresponds to the most stable state with a peroxo 1^1A_1 state lying 9 kcal/mol higher in energy and with an energy barrier around 12 kcal/mol for the superoxo to peroxo transformation. These results are in qualitative agreement with previous work on $[CoO_2]^q$, where this inversion occurred, nevertheless, at $q = 3+$.[1] Although a detailed discussion of the electronic and bonding properties responsible for the relative peroxo to superoxo stability has been given previously,[1,17] It is appropriate to mention at this point that the argument is based on Walsh diagrams for the distortion sequence, constructed with the aid of the valence molecular orbitals calculated for different oxidation numbers (this argument is used at the end of this section to justify the stable peroxo configuration found in $[NiO_2]^0$). There are numerous transition metal–O_2 complexes supporting this picture,[17] and this effect has a definite experimental basis. Quantitatively, the absolute value of the thermodynamic stability differences Δ ($\Delta = |E_p - E_s|$, where E_p and E_s correspond to the energy at the points P and S in Figure 1) among the most stable peroxo and superoxo states is larger than 9 kcal/mol for all the NiO_2 systems studied in this work. These relatively large values of Δ and E_a found in all the Ni–O_2 adducts studied (at least 9 kcal/mol for Δ and 12 kcal/mol for E_a) indicate that only the most stable geometry would be significantly populated at moderate temperatures, i.e., the dioxygen TPD spectra of these nickel systems would present only one peak. This type of behavior has been found in connection with the TPD spectra of O_2 adsorbed on Ni(II) ion-exchanged Y-type zeolites.[18] The relation among this chemical environment and the Ni–O_2 models studied are currently under investigation.

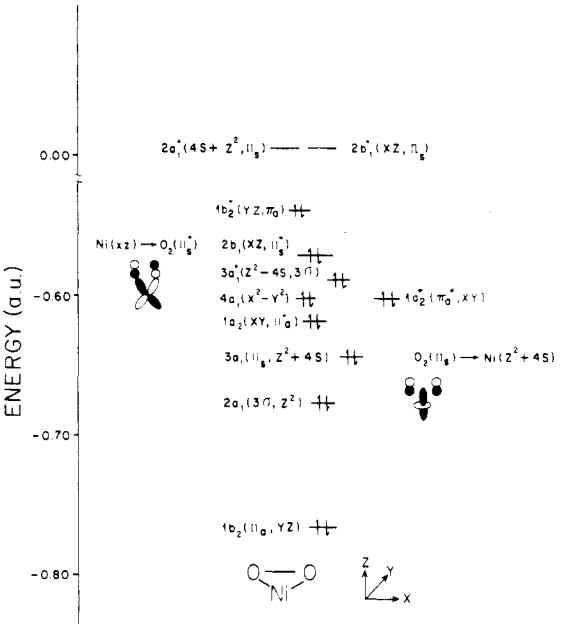

Figure 2. Orbital energy diagram for the $^1A_1$ ground state of $[NiO_2]^0$.

TABLE IV: O_2 Activation Properties of the Most Stable Deformation States of NiO_2

system[a]	$O_2(\pi^*)$ electron population[b]	charge on O_2, e	Mulliken bond order	bond length, Å	oxidtn state in Boca's formulation[c]
$^1A_1[NiO_2]^0$	2 + 0.98	−0.34	0.94	1.28	$[Ni^I(O_2)^-]^0$
$2^1A'[NiO_2]^{2+}$	2 − 0.33	+0.59	1.14	1.23	$[Ni^{II}(O_2)^0]^{2+}$

[a] C_{2v} designation is used for the peroxo and C_s for the superoxo states. [b] For free O_2: Mulliken bond order = 1.31, bond length = 1.205 Å, and Boca's index = 2. [c] Reference 19.

The molecular orbital diagram for the peroxo $^1A_1$ ground state of the neutral Ni–O_2 system is shown in Figure 2, where the subscripts s and a are used to indicate the symmetric or antisymmetric character with respect to the $x0z$ plane of symmetry, respectively, and the asterisk is used to indicate the Co–O_2 antibonding character of the level. We have also indicated the main Ni and O_2 components of each molecular orbital following its group symmetry C_{2v} designation (we have also neglected the Ni(4p) mixing because it is relatively small). The stable side-bonded geometry of this system follows from the dominant role of the valence $1b_2^*(yz,\pi)$ antibonding orbital, which is continuously destabilized along the distortion coordinate, and it correlates to the more antibonding $\pi^*(yz,\pi)$ level in the linear structure.[1,17] Perturbation theoretic reasoning behind correlation diagrams such as in Figure 2 is frequently invoked,[17] i.e., an orbital distortion Walsh diagram for the highest occupied level is needed at this point to corroborate the above assertion. The calculated orbital distortion-energy curve for the $1b_2^*$ level is, nevertheless, identical with the one depicted in Figure 6 of the previous work on Co–O_2[1] (see also Figure 7 in ref 17), which clearly favors a peroxo stable geometry.

Dioxygen Activation Properties of $[NiO_2]^q$

The $O_2(\pi^*)$ electron population described by the $\chi(\pi)$ index introduced by Boca[19] together with the charge, Mulliken bond order, and bond length of coordinated O_2, for the most stable deformation states of $[NiO_2]^q$ ($q = 0, 2+$), are displayed in Table IV. These properties show that the degree of O_2 activation

(16) Blomberg, M. R. A.; Siegbahn, P. E. M.; Strich, A. *Chem. Phys.* **1985**, *97*, 287.
(17) Hoffmann, R.; Chen, M. M. L.; Thorn, D. L. *Inorg. Chem.* **1977**, *16*, 503.
(18) Iwamoto, M.; Maruyama, K.; Yamazoe, N.; Seiyama, T. *J. Chem. Soc., Chem. Commun.* **1976**, 615.
(19) Boca, R. *Coord. Chem. Rev.* **1983**, *50*, 1.

TABLE V: Dissociation States of $[NiO_2]^0$

state[a]	config	equil bond length, Å Ni–O	O–O	total energy, au	charge on the oxygen atoms, e
$^1A_2$	α-$5a_1 1a_2 3b_1 2b_2$ β-$4a_1 2a_2 3b_1 2b_2$	1.70	2.87	−73.4264	−0.217
$^3B_2$	α-$5a_1 2a_2 3b_1 2b_2$ β-$5a_1 1a_2 2b_1 2b_2$	1.72	3.38	−73.4182	−0.165

[a] See Figure 3.

decreases when q increases from 0 to 2+. In terms of Boca's formulation, indicated by last column of Table IV, the activation of O_2 decreases when the oxidation state of Ni increases from Ni(0) to Ni(II). These results are in agreement with previous work,[1] where a decrease in the O_2 activation is also observed in going from Co(0) to Co(III). The $^1A_1[NiO_2]^0$ system possesses an approximate π^{*3} electron configuration, which represents an increment of one electron with respect to the π^{*2} orbital occupation in free O_2. This activation is evidenced in Table IV by an increase in the calculated O_2 bond length from 1.21 to 1.28 Å in going from free O_2 to $[NiO_2]^0$. In contrast, the $2^1A[NiO_2]^{2+}$ system is slightly O_2 activated as revealed by the small change in the O_2 bond length and $O_2(\pi^*)$ orbital occupation with respect to free O_2.

The molecular orbital diagram shown in Figure 2 can be also used to describe the dioxygen activation properties of the $^1A_1$ peroxo ground state of $[NiO_2]^0$ in terms of the main interactions between Ni($4s^1$,$3d^7$) and O_2. In the lower energy region of the spectrum the main bonding interactions corresponds to the $3a_1(\pi, z^2+4s)$ orbital, and it represents the major electronic mechanism for the donation of 0.64 electron from O_2 to the Ni atom. In the upper energy region the $2b_1(xz,\pi^*)$ orbital represents the main π back-bonding interaction responsible for the donation of 0.98 electron from Ni to dioxygen. Since the σ donation drives away electron density from the bonding $O_2(\pi)$ orbital and the π back-bonding increases the $O_2(\pi^*)$ electron population, they are both responsible for the observed activation of coordinated dioxygen, in agreement with previous calculations on the neutral Co–O_2 adduct.[1] Recent ab initio calculations of Blomberg et al.[16] also describe the weakening of the O_2 bond in terms of the charge donation into the Ni(4s) from the $O_2(\pi)$ orbitals and back-donation from the Ni(3d) into the $O_2(\pi^*)$ orbitals, although they seem to completely neglect the Ni(3d) orbital participation in the σ donation interaction.

Dissociation Properties of Coordinated O_2

The above calculations for the $^1A_1$ peroxo state of $[NiO_2]^0$ illustrate the dioxygen activation in terms of the O–O bond softening under coordination with nickel. This activated "molecular" state is taken to be the precursor for the process of dissociation of O_2 in terms of the opening of the O–Ni–O bond angle. In geometry optimization calculations, the variation in energy with the dissociation angle for the most stable states of the neutral Ni molecule is shown in Figure 3. The equilibrium bond distances, total energy, and charge on the dioxygen for the most stable "dissociated" state are shown in Table V.

The dissociation curves depicted in Figure 3 for the $[NiO_2]^0$ system indicate that the molecular $^1A_1$ state is lower in energy than the $^1A_2$ and $^3B_2$ dissociated states. It also indicates a thermal barrier of at least 112 kcal/mol for the dissociation process indicated by the path M → C → D in Figure 3. This barrier is very high, although in agreement with previous calculations for Co–O_2,[1] Fe–O_2,[20] and Ni–O_2[16] and the experimental results of Huber and Ozin[5] indicating that the dioxygen dissociation on a single metal atom is not a likely process.

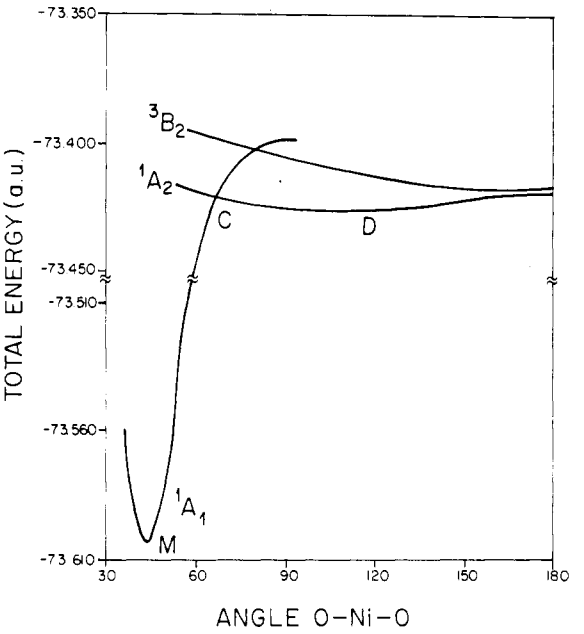

Figure 3. Energy of $[NiO_2]^0$ as a function of the O–Ni–O bond angle for the $^1A_1$ molecular state and the dissociation states listed in Table V.

Conclusions

The results obtained for the M–O_2 (M = Ni, Co) interactions show unambiguously that the modified CNDO-UHF procedure used constitutes an adequate method for the correct interpretation of experimental data, provided that (a) the state of minimum energy for a given configuration is maintained when the molecule undergoes a structural change along a given reaction coordinate and (b) the poor CNDO estimates of the binding energies are improved by an adequate parametrization, which reproduces the equilibrium bond lengths and bond energies of the diatomic species involved.

In particular, this scheme gave the expected changes in the distortion properties of Ni–O_2 and Co–O_2, i.e., the transformation from peroxo to superoxo most stable conformer when the oxidation number increased from Ni(0), Co(0) to their highest value Ni(II), Co(III), with a corresponding decrease in the O_2 activation. The lowest activation energy calculated corresponded to 112 kcal/mol, which suggests that dissociative adsorption of O_2 on a single atom is not a likely process.

Registry No. NiO, 1313-99-1; NiO^{2+}, 115290-66-9; Ni, 7440-02-0; O_2, 7782-44-7.

(20) Blyholder, G.; Head, J. *Ruette*, F. *Inorg. Chem.* **1982**, *21*, 1539.